

---

---

# Review on Production of $^{89}\text{Zr}$ in a Medical Cyclotron for PET Radiopharmaceuticals

Azahari Kasbollah<sup>1,2</sup>, Peter Eu<sup>3</sup>, Simon Cowell<sup>1</sup>, and Pradip Deb<sup>1</sup>

<sup>1</sup>Discipline of Medical Radiations, School of Medical Sciences, RMIT University, Victoria, Australia; <sup>2</sup>Malaysian Nuclear Agency, Ministry of Science, Technology and Innovation (MOSTI), Putrajaya, Malaysia; and <sup>3</sup>Peter MacCallum Cancer Centre, Victoria, Australia

---

This article is intended to provide an overview of the production and application of  $^{89}\text{Zr}$  for the professional development of nuclear medicine technologists. It outlines the cyclotron targeting, separation and labeling options, and techniques for the preparation of the radionuclide  $^{89}\text{Zr}$  (half-life, 78.4 h [3.3 d]) used in PET. Unlike the commonly used  $^{18}\text{F}$ -FDG, with a 109.7-min half-life, the longer half-life of  $^{89}\text{Zr}$  makes it possible to use high-resolution PET/CT to localize and image tumors with monoclonal antibody radiopharmaceuticals and thus potentially expand the use of PET. **Methods:** This paper briefly reviews the cyclotron technique of  $^{89}\text{Zr}$  production and outlines the range and preparation techniques available for making  $^{89}\text{Y}$  targets as a starting material. It then discusses how cyclotron-produced  $^{89}\text{Zr}$  can be separated, purified, and labeled to monoclonal antibodies for PET/CT of specific tumors. **Results:** We argue that knowledge and understanding of this long-lived PET radionuclide should be part of the professional development of nuclear medicine technologists because it will lead to better patient outcomes and potentially increase the pool of collaborators in this field of research.

**Key Words:** positron emission tomography (PET); monoclonal antibodies; yttrium solid target;  $^{89}\text{Zr}$  radionuclide; radiolabeling

**J Nucl Med Technol 2013; 41:35–41**

DOI: 10.2967/jnmt.112.111377

---

**T**he Nobel Prize in Chemistry won by George de Hevesy in 1943 for the development of the tracer principle used in nuclear medicine is possibly one of the most significant achievements of the 20th century (1). The introduction of cyclotron and PET technology into clinical medicine greatly improved the management of patients with cancer and other diseases, and the development of combined imaging with PET/CT has substantially improved the effectiveness of this modality (2). A radiopharmaceutical

(radiotracer) is a radioactive compound used for the diagnosis and therapeutic treatment of human diseases. It is composed of 2 parts: a radionuclide, which is a radioactive isotope that can be injected safely into the body, and a pharmaceutical, which acts as a carrier molecule delivering the isotope to the area to be treated or examined within the body. For a radiotracer to be used safely in humans, for imaging or therapy, it must meet high standards for quality that include chemical and radiochemical purity, sterility, and freedom from pyrogenic material. For functional nuclear medicine imaging, there are few ideal radiopharmaceuticals (3). Table 1 outlines the ideal diagnostic radiopharmaceutical for imaging. The ability to measure regional biochemical function requires a careful design process with these principles in mind. However, in reality it is not possible to meet all of these criteria. For example, all decay processes involve the emission of particles, as in the case of the pure  $\gamma$ -emitters, which have Auger electrons emitted during some fraction of the decays. Thus, in addition to the quest for an ideal radiopharmaceutical in the development of a biochemical probe, the following 3 factors must be considered (4): the radiotracer must be able to bind preferentially to a specific site, the radiotracer must be sensitive to minor changes in biochemistry, and if possible, the specific biochemical change should be a function of a specific disease that matches that sensitivity.

Many radiotracers have been synthesized to probe metabolic turnover such as oxygen consumption, glucose utilization, and amino acid synthesis. Enzymatic activity, neurotransmission, receptor density, and occupancy have all been measured through appropriately designed radiotracers. It should be emphasized that the development of radiotracers for PET fundamentally violates rule 2(a) in Table 1 for the ideal diagnostic radiopharmaceutical for imaging because PET radionuclides emit  $\beta^+$  particles by nature. However, the resulting coincident  $\gamma$ -rays from the  $\beta^+$  annihilation form the basis for the technique.

Additionally, in consideration of the above principles, a plan must be considered on how to insert the radionuclide into the molecule at a point in the synthetic process with minimal handling yet late enough in the synthesis to minimize loss due to chemical yield and radioactive decay. For these reasons, the preparation of radiopharma-

---

Received Jul. 19, 2012; revision accepted Nov. 29, 2012.

For correspondence or reprints contact: Azahari Kasbollah, Discipline of Medical Radiations, School of Medical Sciences, RMIT University, P.O. Box 71, Bundoora, Victoria 3083, Australia.

E-mail: azahari@nuclearmalaysia.gov.my

Published online Jan. 17, 2013.

COPYRIGHT © 2013 by the Society of Nuclear Medicine and Molecular Imaging, Inc.

**TABLE 1**  
Properties of Ideal Diagnostic Radiopharmaceutical for Imaging

Properties	Notes
1. Easy availability	Be readily available at low cost
2. Particle emission	Diagnostic purpose: be a pure $\gamma$ -emitter—that is, have no particle emission such as $\alpha$ and $\beta$ because these contribute radiation dose to patient without providing diagnostic information Therapeutic purpose: have particle emission such as $\alpha$ and $\beta$ because these are useful for damaging abnormal cells
3. High target-to-nontarget activity ratio	Provide maximum efficacy in diagnosis (therapy), and minimize radiation dose to patient
4. Proper metabolic activity	Possess proper metabolic activity—that is, follow or be trapped in metabolic process of interest

ceuticals requires good planning and techniques that are not encountered by traditional synthetic chemistry.

### PET and Immuno-PET

In the beginning of the 1950s, Wrenn et al. proposed the use of coincidence techniques to image positron-emitting radionuclides to study  $^{64}\text{Cu}$  in brain tumors using opposing sodium iodine detectors (5). Soon, the Anger camera was launched onto the market in 1954 and was quickly applied to positron emitters (6). Na(I) detectors with coincidence capabilities were used in clinical investigations during the 1960s (7). In the beginning of the 1970s, an important progression in this field occurred with the introduction of the tomography principle (8), leading to the development of the PET technique. Thus, PET arose from the outcome of 2 Nobel Prize awards, the tracer principle (de Hevesy in Chemistry in 1943) and the tomographic principle (Godfrey N. Hounsfield and Allan M. Cormack in Medicine in 1979) (1).

PET is a nuclear medicine technique that produces a 3-dimensional image or map of functional processes in the body. The system detects pairs of  $\gamma$ -rays emitted indirectly by a positron-emitting radioisotope, which is introduced into the body on a metabolically active molecule. The PET radioisotope sends out a positron that eventually finds an electron, forming a complex atom called positronium that rapidly decays and emits 2 annihilation photons. PET cameras detect the 511-keV photons that are emitted at  $180^\circ$  from each other and enable the production of a 3-dimensional image (1). PET images generate physiologic and functional information for the observer, but the anatomic structures are sometimes hard to distinguish. Therefore, most new PET scanners come as dual-imaging devices known as PET/CT scanners, enabling the functional information from PET to be displayed with the structural information from CT.

Immuno-PET, a combination of PET and monoclonal antibodies (mAbs), is an attractive novel tumor imaging option because it has the potential to improve diagnostic tumor characterization by combining the high sensitivity and resolution of PET/CT with the specificity of a mAb localization (9). In fact, each mAb that targets a specific tumor cell is a candidate for use in immuno-PET, allowing

for the development of a new generation of mAb-based imaging probes.

PET also has the potential for quantification of molecular interactions, which is especially attractive when immuno-PET is used as a prelude to therapy with one of the approved mAbs. In a personalized therapeutic approach, immuno-PET enables the confirmation of tumor targeting and the quantification of mAb accumulation. Immuno-PET might also play a role in the efficient selection, characterization, and optimization of novel high-potential mAbs or mAb-conjugate candidates for diagnosis and therapy (10).

### $^{89}\text{Zr}$ Radioisotope

In more recent years, there has been increased interest in such nonconventional positron emitters as  $^{89}\text{Zr}$ . Since the introduction of the long-lived positron emitter  $^{89}\text{Zr}$  as a residualizing radionuclide for immuno-PET, procedures have been developed for large-scale production of  $^{89}\text{Zr}$  and its stable coupling to mAbs (11,12). To have a successful diagnostic in PET for solid tumors, a radionuclide's half-life must be suitable for target accumulation and nonspecific clearance. The most commonly used PET radionuclides such as  $^{18}\text{F}$  and  $^{11}\text{C}$ , which have short half-lives of 109.7 and 20 min, respectively, are not suitable for detection of solid tumors because they would undergo appreciable radioactive decay before reaching the center of the tumor (13). Although  $^{18}\text{F}$ -FDG is used to find tumors because the sugar molecule targets quickly, the clearance time of radioimmunoconjugates is relatively long; thus, good target-to-blood ratios are not achieved within 24 h after administration with the relatively short half-life of  $^{18}\text{F}$ .  $^{124}\text{I}$ , on the other hand, has a half-life of 4.2 d, but there are substantial isotopic enrichment costs involved and the added danger of exposure of thyroid tissue (in particular) to free radioactive iodine.  $^{89}\text{Zr}$  has ideal physical characteristics for immuno-PET and has been suggested for use in quantifying slow processes and deposition of mAbs in tissue and tumor. Because intact antibodies need around 2–4 d to penetrate to a solid tumor, the half-life of  $^{89}\text{Zr}$  (3.3 d), with 23% positron emission ( $\beta^+$ ) decay and 77% electron capture, is compatible with the time needed for these mAbs to achieve optimal tumor-to-nontumor uptake ratios (14). In contrast, to achieve good visualization, a large dose—

which is costly and, more important, dangerous to the patient with regard to radiation exposure—would need to be administered (15). The relatively low translational energy of the emitted positron for  $^{89}\text{Zr}$  results in high-resolution images comparable to those observed using the  $^{18}\text{F}$  and  $^{64}\text{Cu}$  radionuclides (16–18). Table 2 breaks down the characteristics of selected PET radionuclides for radioimmunoimaging (19).  $^{89}\text{Zr}$  has good  $\gamma$ -energies, allowing imaging using PET scanners. Without this property, visualization of the antibodies would not be possible. Another factor to consider is the daughter nuclides formed by the positron decay of zirconium:  $^{89}\text{Y}$ . This radionuclide is stable and will not cause any damage in vivo (20). The biggest challenges preventing  $^{89}\text{Zr}$  from becoming a widely used radioisotope for immuno-PET are its limited availability and the high-energy  $\gamma$ -emission at 908.97 keV, which may limit the radioactive dose that can be administered to patients. Moreover, a free  $^{89}\text{Zr}$  can target to bone marrow instead of solid tumor (21). So  $^{89}\text{Zr}$  must be well bonded with mAbs or other pharmaceuticals for the radiotracer to securely reach the center of the tumor.

## PRODUCTION PROCEDURES OF $^{89}\text{Zr}$ RADIOISOTOPE

### Target Materials and Irradiation

A cyclotron target is a container into which the target material to be irradiated is introduced. Target material can be gas, liquid, or solid, depending on the radioisotope of interest. Targets specially designed for the production of the most common positron emitters ( $^{18}\text{F}$ ,  $^{11}\text{C}$ ,  $^{13}\text{N}$ , and  $^{15}\text{O}$ ) are a standard feature in conventional cyclotrons, and this design has been optimized over many years. The  $^{89}\text{Zr}$  radioisotope is an example of a nonconventional positron emitter that has limited commercial availability but can be produced from a starting material of  $^{89}\text{Y}$  solid target. The target is usually bombarded in a cyclotron with a certain beam current and time to finally produce the  $^{89}\text{Zr}$  radioisotope.

### Yttrium Target for Production of $^{89}\text{Zr}$

Yttrium target is an example of solid target material that is introduced into a cyclotron container for irradiation to

produce the  $^{89}\text{Zr}$  radioisotope. There are a few types of, and techniques for preparation of, yttrium solid target as a starting material.

**Yttrium Foil.** Dejesus and Nickles used water-cooled yttrium foils to produce  $^{89}\text{Zr}$  via the (p,n) reaction on  $^{89}\text{Y}$  with 11-MeV protons (14). The target was bombarded with protons (1-cm-diameter beam) typically for 2 h, with a beam current of 10  $\mu\text{A}$ . Then the target was dissolved in concentrated HCl (5 mL) as reported by Link et al. (these authors found that HCl gave less insoluble material) (22).

**Yttrium Pellet.** Zweit et al. described the production of no-carrier-added  $^{89}\text{Zr}$  for PET from deuteron irradiation of natural yttrium targets (23). The target material of natural yttrium powder (100%  $^{89}\text{Y}$ ) was pressed into 10-mm-diameter pellets ranging in thickness from 240 to 340  $\text{mg}/\text{cm}^2$ , which were placed in the target holders. Then the pellets were covered with high-purity aluminum foil 0.005–0.36 mm thick depending on the incident deuteron energy required. The beam currents used were 3 and 5  $\mu\text{A}$ , with irradiation times of 12 and 20 min, respectively. The energy window used for the  $^{89}\text{Y}(\text{d},2\text{n})^{89}\text{Zr}$  reaction was from 16 to 7 MeV. This window was considered to be optimum to minimize the production of the long-lived  $^{88}\text{Zr}$  formed by the  $^{89}\text{Y}(\text{d},3\text{n})$  reaction with a threshold energy of 15.5 MeV.

**Yttrium Sputtering.** A different  $^{89}\text{Y}$  target can be prepared using the sputtering technique. Meijs et al. reported that the target can be prepared by sputtering an yttrium layer (25  $\mu\text{m}$ ) on a copper support. In this process, the yttrium atoms are ejected as a result of momentum transfer between accelerated argon ions and the yttrium source. The yttrium atoms cross a vacuum chamber ( $7 \times 10^{-3}$  torr) and finally deposit on the copper support (11).

**Yttrium Deposition.** Films of yttrium are usually produced by vapor deposition, dry processes, and sputtering, but electroplating would be advantageous in view of the cost and productivity. Kumbhar and Lokhande reported the electrodeposition of yttrium from a nonaqueous (ethanol) bath (24). The distance between anode and cathode was 0.2 cm. Deposition was performed under unstirred conditions and in the potentiostatic mode. The study indicated that at

**TABLE 2**  
Characteristic of Selected PET Radionuclides for Radioimmunoimaging (19)

Radionuclide	Half-life	Production	positron emission		$\gamma$ -energies		Intrinsic spatial resolution loss (mm)
			maximum energy ( $\beta^+_{\text{max}}$ ) MeV	$\beta^+$ yields (%)	MeV	Yields (%)	
$^{89}\text{Zr}$	78.4 h	$^{89}\text{Y}(\text{p},\text{n})^{89}\text{Zr}$	0.909	23	—		1.0
		$^{89}\text{Y}(\text{d},2\text{n})^{89}\text{Zr}$					
$^{124}\text{I}$	100.2 h	$^{124}\text{Te}(\text{p},\text{n})^{124}\text{I}$	2.14	24	0.60	61	2.3
		$^{124}\text{Te}(\text{d},2\text{n})^{124}\text{I}$					
		$^{125}\text{Te}(\text{p},2\text{n})^{124}\text{I}$					
$^{18}\text{F}$	1.83 h	$^{20}\text{Ne}(\text{d},\alpha)^{18}\text{F}$	0.63	97	0.14	41	0.7
		$^{18}\text{O}(\text{p},\text{n})^{18}\text{F}$					

room temperature, the thickness of the deposit increases linearly with time up to 1 h. The effect of temperature showed that good-quality uniform white–gray deposits could be obtained at up to 45°C. Sadeghi et al. reported 2 special sedimentation methods to deposit a thick layer of yttrium oxide ( $Y_2O_3$ ) on copper substrate for the production of  $^{89}Zr$  (25). A thick layer of  $Y_2O_3$  was deposited on the copper substrate (surface area, 11.69 cm<sup>2</sup>) by ethyl cellulose and methyl cellulose methods. The target was irradiated with up to a 20- $\mu$ A current with 13-MeV protons, and no degradation was observed.

### Production of $^{89}Zr$

There are 2 nuclear reactions that have been explored for the production of  $^{89}Zr$  and typically by cyclotron bombardment of  $^{89}Y$ . The first and most commonly used is the  $^{89}Y(p,n)^{89}Zr$  reaction (14,26), because a higher yield of  $^{89}Zr$  can be produced from  $^{89}Y$ , which is 100% naturally abundant in the earth's crust. Typically in this reaction, a proton beam with 14- to 14.5-MeV energy is used to bombard an yttrium foil solid target for 2–3 h with a 65- to 80- $\mu$ A beam current. Because yttrium has only 1 stable isotope and the product can be made relatively pure at low energy, this reaction is ideal for the production of  $^{89}Zr$ . The other reaction that has been used for the production of  $^{89}Zr$  in the cyclotron is the  $^{89}Y(d,2n)^{89}Zr$  reaction (23). Usually in this reaction, an yttrium pellet is used and irradiated with a 16-MeV deuteron beam, and  $^{89}Zr$  can be purified and separated from the target by ion-exchange chromatography. Theoretically, all the bifunctional chelating agents, such as diethylenetriamine pentaacetic acid (DTPA) and 1DOTA derivatives, for  $^{111}In$  and  $^{90}Y$  labeling can be used for  $^{89}Zr$  labeling of biomolecules (27). The dominant oxidation number of zirconium is +4—which, when combined with a relatively small size, leads to an extensive hydrolyzed aqueous chemistry with a largely covalent nature. Donor ligands containing oxygen, nitrogen, and chloride are especially stable, commonly creating complexes with coordination numbers of 7, 8, or higher. High coordination numbers (7 and 8) are characteristic of zirconium complexes, and the ligands are normally labile, resulting in the great variety of stereochemistries. Different radiometals have significant differences in their coordination chemistry. Because the radiometal chelate can significantly affect biologic properties, the biodistribution of a target-specific radiopharmaceutical can be systematically changed either by modifying the coordination environment around the radiometal with a variety of chelators or by using various coligands if the radiometal chelate contains 2 or more ligands (28).

### Purification of $^{89}Zr$

One of the biggest challenges preventing  $^{89}Zr$  from becoming a widely used radioisotope for immuno-PET is the process to rid it of other impurities. Bombardment of the yttrium solid target results in a large number of radiochemical impurities, along with the radionuclide impurity of trace  $^{88}Zr$  (~0.01%). The target itself contains

a copper metal backbone and trace amounts of titanium, iron, and gadolinium. After bombardment, trace products of  $^{65}Zn$ ,  $^{48}V$ ,  $^{56}Co$ , and  $^{156}Tb$  are formed to the trace metals located on the target (12). These unwanted impurities must be separated from  $^{89}Zr$  because they might compete in the labeling step with the antibodies (11). Purification of  $^{89}Zr$  usually involved the separation process of  $^{89}Zr$  radionuclide from its impurities and starting materials, followed by elution of the radionuclide from the retention column. The  $^{89}Zr$  can be dissolved in hydrochloric acid and separated from other radioisotopes and the target material on an ion-exchange column (11,23). In some cases, a wet chemical extraction preceded the ion-exchange separation (22). It was found that the hydroxamic function had high specific affinity for zirconium. Even at high acid concentrations—that is, at concentrations higher than 1 M HCl—zirconium is able to form complexes with hydroxamates, whereas its impurities are not (23). The latest method of removing these impurities uses a hydroxamate resin column (12,20). The hydroxamate resin column can produce 99.9% carrier-free  $^{89}Zr$ ; however, the extraction technique proved to be counterintuitive to the purpose of purification (14). Because the  $^{89}Zr$  is ionically bonded to the column, a stronger anion exchanger is needed to remove it. It was found that the most convenient solution for transchelating the  $^{89}Zr$  from the column was oxalic acid in a concentration of at least 0.5 M (11). Verel et al. have successfully transchelated 97% of the total activity from the hydroxamate column using 1 M oxalic acid over 5 separate elutions, with an initial 40% yield in the first 2 elutions and a purity of more than 99.9% (12).

However, there are some issues that arise with oxalic acid as an extraction chemical for purifying  $^{89}Zr$ . Oxalic acid is highly toxic to the human body, causing blood decalcification—which is detrimental to neural and muscle function—as well as renal tubule obstruction via calcium oxalate precipitation (20). Hence, the *in vivo* use of  $^{89}Zr$ -bound oxalic acid cannot be considered. It was demonstrated that removing the oxalic acid required the use of another strong anion-exchange column and the flushing of a large volume of water through the column, followed by chloride exchange using HCl. The resultant acid solution could then be boiled off at 110°C under a continuous stream of argon and reconstituted in 0.9% NaCl solution (12). After this purification process, a carrier-free, purified  $^{89}Zr$  was then able to be bound to a mAb desferrioxamine complex (29).

### Radiolabeling of Antibodies with $^{89}Zr$

Over the past 20 y, attempts have been made to label proteins and antibodies with  $^{89}Zr$  using DTPA derivatives and porphyrins as chelating agents (22,30), as well as desferrioxamine conjugates (31,32). The process incorporates desferrioxamine groups onto mAbs in a 2-step procedure in which maleimide groups were incorporated into the protein and the thioester of desferrioxamine that was formed was

further converted to a free thiol with hydroxylamine to facilitate reaction with the maleimide groups of the antibody, with subsequent radiolabeling with  $^{89}\text{Zr}$  (31,32). In 2010, Perk et al. introduced the novel bifunctional chelating agent *p*-isothiocyanatobenzyl-desferrioxamine B (Df-Bz-NCS) for the facile radiolabeling of mAbs with  $^{89}\text{Zr}$  for immuno-PET. They also compared its performance in  $^{89}\text{Zr}$  for immuno-PET with the reference bifunctional TFP-*N*-sucDf (12) and demonstrated that the novel Df-Bz-NCS allowed the efficient and easy preparation of optimally performing  $^{89}\text{Zr}$ -labeled mAbs, facilitating further exploration of  $^{89}\text{Zr}$  immuno-PET as an imaging tool, with oxalic acid being used to extract the  $^{89}\text{Zr}$  from the hydroxamate resin column (33). The step-by-step procedure was then described for the facile radiolabeling of mAbs or other proteins with  $^{89}\text{Zr}$  using Df-Bz-NCS. First, Df-Bz-NCS was coupled to the lysine-NH<sub>2</sub> groups of a mAb at pH 9.0 (premodification), and then it was purified using gel filtration. Next, the pre-modified mAb was labeled to  $^{89}\text{Zr}$  at room temperature by the addition of  $^{89}\text{Zr}$ -Zr-oxalic acid solution, and then it was purified using PD-10 column gel filtration to remove the unlabeled product and oxalic acid from the labeled compound (34).

#### In Vitro and In Vivo Studies of the $^{89}\text{Zr}$ Complex

After the mAb has been successfully labeled with  $^{89}\text{Zr}$ , it is usual for the complex to be studied in vitro and in vivo to evaluate its effectiveness in binding with the specific tumors and the potential effectiveness of the complex in PET for detecting and monitoring treatment responses. Chopra (35) determined the in vitro binding characteristics of  $^{89}\text{Zr}$ -trastuzumab and  $^{111}\text{In}$ -trastuzumab using SKVO3 cells (human ovarian cancer cell line over-expressing human epidermal growth factor receptor 2 [HER2]) and GLC4 cells (human small cell cancer cell line, HER2-negative) by a flow cytometric method (36). Little change in the immunoreactive fraction of  $^{89}\text{Zr}$ -trastuzumab was noted during 7 d of storage either at 4°C (from 0.87 to 0.85 ± 0.06) or at 37°C in human serum (from 0.87 to 0.78 ± 0.01). A similar trend in the immunoreactivity of  $^{111}\text{In}$ -trastuzumab was reported at the 2 storage temperatures.

Once in vitro studies are completed, the radiopharmaceutical can be assessed with in vivo studies using animals such as mice (31,33), followed by human studies (37,38). Basically, before the targeted imaging technique can be used in humans, it is necessary to evaluate the effectiveness of the trastuzumab-*N*-sucDf- $^{89}\text{Zr}$  in animals to evaluate biodistribution, tumor concentration, and PET detection capabilities. Sampath et al. used BALB/c nude mice, that had received the human breast cancer tumor cell line SKBR-3 transplanted into the dorsal region of the left flank, to look at the biodistribution and concentration of trastuzumab-*N*-sucDf- $^{89}\text{Zr}$  in the tumor site and the ability of the PET scanner to detect tumors using this complex. The tumors were grown to 0.5–0.8 cm in diameter, and the mice were

then injected via the tail vein with 200 μg of trastuzumab-*N*-sucDf- $^{89}\text{Zr}$  and imaged right after injection and 2–48 h after injection (39). Our preliminary results on biodistribution and imaging experiments showed a selective accumulation of  $^{89}\text{Zr}$ -Df-trastuzumab in tumor-bearing mice (Fig. 1). The introduction of a mouse model allows the radionuclide to be assessed in the context of a full biologic system (19) and as a preliminary step in translating bench research into a means of identifying and perhaps subsequently treating cancer in human subjects.

#### PET of $^{89}\text{Zr}$ -Labeled mAbs

The most common applications of PET are in the field of oncology, cardiology, and neurology. Since the introduction of the long-lived positron emitter  $^{89}\text{Zr}$  as a residualizing radionuclide for immuno-PET, procedures have been developed for the large-scale production of  $^{89}\text{Zr}$  and its stable coupling to mAbs (12,20).

A feasibility study has been performed to determine the optimal dosage and time of imaging of the mAb  $^{89}\text{Zr}$ -trastuzumab to enable PET of HER2-positive lesions. Fourteen patients with HER2-positive metastatic breast cancer received 37 MBq of  $^{89}\text{Zr}$ -trastuzumab using 1 of 3 doses (10 or 50 mg for those who were trastuzumab-naive and 10 mg for those who were already on trastuzumab treatment). The patients underwent at least 2 PET scans between days 2 and 5. The results of the study showed that the best time for assessment of  $^{89}\text{Zr}$ -trastuzumab uptake by tumors was 4–5 d

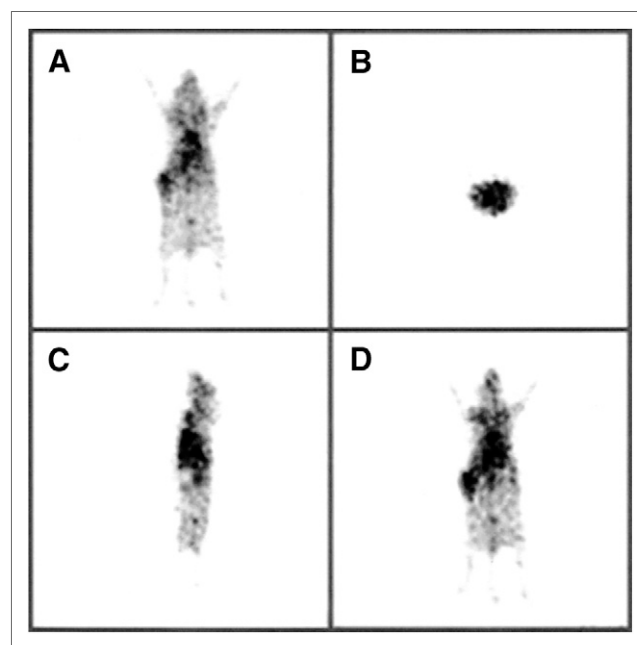


**FIGURE 1.** PET images of HER2-expressing LS174T tumor-bearing mouse (tumor size, 180 mm<sup>3</sup>) at 24 h after injection with 1.85 MBq of  $^{89}\text{Zr}$ -Df-trastuzumab using small-animal PET facility at Peter MacCallum Cancer Centre, Melbourne, Victoria, Australia. Four views are shown: posterior (A), slice view (B), side view (C), and posterior (D).

after the injection (38). For optimal PET scan results, trastuzumab-naïve patients required a 50-mg dose of  $^{89}\text{Zr}$ -trastuzumab, and patients already on trastuzumab treatment required a 10-mg dose. The accumulation of  $^{89}\text{Zr}$ -trastuzumab in lesions allowed PET imaging of most of the known lesions and some that had been undetected earlier. The relative uptake values (mean  $\pm$  SEM) were  $12.8 \pm 5.8$ ,  $4.1 \pm 1.6$ , and  $3.5 \pm 4.2$  in liver, bone, and brain lesions, respectively, and  $5.9 \pm 2.4$ ,  $2.8 \pm 0.7$ ,  $4.0 \pm 0.7$ , and  $0.20 \pm 0.1$  in normal liver, spleen, kidneys, and brain tissue, respectively. PET scanning after administration of  $^{89}\text{Zr}$ -trastuzumab at appropriate doses allowed the visualization and quantification of uptake in HER2-positive lesions in patients with metastatic breast cancer.

Several clinical trials with  $^{89}\text{Zr}$ -labeled mAbs have recently been taking place, such as a study of  $^{89}\text{Zr}$ -trastuzumab for the detection of HER2-positive tumor lesions in breast cancer patients and for the quantification of HER2 expression levels (37). The highest uptake was found in HER2-positive tumors at 144 h after injection (40 percentage injected dose per gram of [%ID/g] tissue for  $^{89}\text{Zr}$ -trastuzumab and 47 % ID/g for  $^{111}\text{In}$ -ITC-DTPA-trastuzumab), compared with 8 % ID/g tissue in HER2-negative control tumors. Liver uptake was low (8–12 %ID/g of tissue). Preliminary results from the first patients in that study showed excellent tumor tracer uptake and a resolution that was much better than that observed in previous SPECT studies with  $^{111}\text{In}$ -trastuzumab (40). In PET, the need for stable chelation chemistry remains an important consideration with this element because uncomplexed and unlabeled radioisotopes localize in the bone and will deliver a high radiation dose to the bone marrow (21).

## CONCLUSION

This review focuses on the long-lived positron emitter  $^{89}\text{Zr}$ , for which the crucial achievements have been obtained to allow broad-scale clinical application of  $^{89}\text{Zr}$  immuno-PET in clinical mAb development and applications.  $^{89}\text{Zr}$  is currently commercially available worldwide for clinical use and protocols for labeling mAbs with  $^{89}\text{Zr}$  as well as preclinical and clinical proof-of-concept studies have been performed showing the safety, better image quality, and potential for accurate quantification of immuno-PET. It is expected in the future that PET imaging with  $^{89}\text{Zr}$ -based tracers will constantly progress, and further efforts are needed to accelerate the translation of more promising  $^{89}\text{Zr}$ -based tracers into clinical use.

## DISCLOSURE

Financial support was provided by the Ministry of Science, Technology and Innovation (MOSTI), Malaysia. No other potential conflict of interest relevant to this article was reported.

## REFERENCES

- Hans Lundqvist ML, Tolmachev V. Positron emission tomography. *Eur J Nucl Med.* 1998;19:537–552.
- Buck AK, Herrmann K, Stargardt T, Dechow T, Krause BJ, Schreyögg J. Economic evaluation of PET and PET/CT in oncology: evidence and methodologic approaches. *J Nucl Med Tech.* 2010;38:6–17.
- Eckelman WC. The status of radiopharmaceutical research. *Int J Rad Appl Instrum B.* 1991;18:iii–vi.
- Ruth TJ. The production of radionuclides for radiotracers in nuclear medicine. *Reviews of Accelerator Science and Technology.* 2009;02:17–33.
- Wrenn FR, GML, Handler P. The use of positron-emitting radioisotopes for the localization of brain tumors. *Science.* 1951;113:525–527.
- Anger HO. Radioisotope camera instrumentation in nuclear medicine. In: Hine, G J ed. *Instrumentation in Nuclear Medicine.* New York, NY: Academic; 1967: 485–552.
- Aronow S. Positron scanning instrumentation in nuclear medicine. In: Hine, G J ed. *Instrumentation in Nuclear Medicine.* New York, NY: Academic; 1967:461–483.
- Phelps ME, Hoffman EJ, Mullani NA, Ter-Pogossian MM. Application of annihilation coincidence detection to transaxial reconstruction tomography. *J Nucl Med.* 1975;16:210–224.
- Lawrentschuk N, Davis ID, Bolton DM, Scott AM. Positron emission tomography (PET), immuno-PET and radioimmunotherapy in renal cell carcinoma: a developing diagnostic and therapeutic relationship. *BJU Int.* 2006;97:916–922.
- Boswell CA, Brechbiel MW. Development of radioimmunotherapeutic and diagnostic antibodies: an inside-out view. *Nucl Med Biol.* 2007;34:757–778.
- Meijs WE, Herscheid JDM, Haisma HJ, et al. Production of highly pure no-carrier added  $^{89}\text{Zr}$  for the labelling of antibodies with a positron emitter. *Appl Radiat Isot.* 1994;45:1143–1147.
- Verel I, Visser GW, Boellaard R, Stigter-van Walsum M, Snow GB, van Dongen GAMS.  $^{89}\text{Zr}$  Immuno-PET: comprehensive procedures for the production of  $^{89}\text{Zr}$ -labeled monoclonal antibodies. *J Nucl Med.* 2003;44:1271–1281.
- Phelps ME. Molecular imaging and its biological applications. *Eur J Nucl Med Mol Imaging.* 2004;31:1544.
- Dejesus OT, Nickles RJ. Production and purification of  $^{89}\text{Zr}$ , a potential PET antibody label. *Int J Rad Appl Instrum [A].* 1990;41:789–790.
- Verel I, Visser GW, Boerman OC, et al. Long-lived positron emitters zirconium-89 and iodine-124 for scouting of therapeutic radioimmunoconjugates with PET. *Cancer Biother Radiopharm.* 2003;18:655–661.
- Nayak TK, Brechbiel MW. Radioimmunoimaging with longer-lived positron-emitting radionuclides: potentials and challenges. *Bioconjugate Chemistry.* 2009;20:825–841.
- Lewis Jason S, Singh Rajendra K, Welch Michael J. Long lived and unconventional PET radionuclides. *Molecular Imaging in Oncology;* 2008:283–292.
- Hohn A, Zimmermann K, Schaub E, Hirzel W, Schubiger PA, Schibli R. Production and separation of “non-standard” PET nuclides at a large cyclotron facility: the experiences at the Paul Scherrer Institute in Switzerland. *Q J Nucl Med Mol Imaging.* 2008;52:145–150.
- Van Dongen GA, Visser GW, Lub-de Hooge MN, De Vries EG, Perk LR. Immuno-PET: a navigator in monoclonal antibody development and applications. *Oncologist.* 2007;12:1379–1389.
- Holland JP, Sheh Y, Lewis JS. Standardized methods for the production of high specific-activity zirconium-89. *Nucl Med Biol.* 2009;36:729–739.
- Bowen H. The biogeochemistry of the elements. In: *Trace Elements in Biochemistry.* London, U.K.: Academic Press. 1966:173–239.
- Link JM, Krohn KA, Eary JF, et al.  $^{89}\text{Zr}$  for antibody labelling and positron tomography. *J Labelled Comp Radiopharm.* 1986;23:1296–1297.
- Zweit J, Downey S, Sharma HL. Production of no-carrier-added zirconium-89 for positron emission tomography. *Int J Rad Appl Instrum [A].* 1991;42:199–201.
- Kumbhar PP, Lokhande CD. Electrodeposition of yttrium from a nonaqueous bath. *Met Finish.* 1995;93:28, 30–31.
- Sadeghi M, Kakavand T, Taghilo M. Targetry of  $\text{Y}_2\text{O}_3$  on a copper substrate for the non-carrier-added  $^{89}\text{Zr}$  production via  $^{89}\text{Y}(p, n)^{89}\text{Zr}$  reaction. *Kerntechnik.* 2010;75:298–302.
- Saha GB, Porile NT, Yaffe L. (p, xn) and (p, pxn) Reactions of Yttrium-89 with 5–85-MeV Protons. *Phys Rev.* 1966;144:962.
- Liu S. Bifunctional coupling agents for radiolabeling of biomolecules and target-specific delivery of metallic radionuclides. *Adv Drug Deliv Rev.* 2008;60:1347–1370.
- Greenwood NN, Earnshaw A. *Chemistry of the Elements.* Oxford, UK: Pergamon Press; 1984.

29. Meijs WE, Herscheid JDM, Haisma HJ, Pinedo HM. Evaluation of desferal as a bifunctional chelating agent for labeling antibodies with Zr-89. *Int J Rad Appl Instrum [A]*. 1992;43:1443–1447.
30. Ali SA, Shankland EG. Radiochemical synthesis of <sup>89</sup>Zr-porphyrin for positron label of monoclonal antibodies. *J Labelled Comp Radiopharm*. 1991;30:326.
31. Meijs WE, Haisma HJ, Klok RP, et al. Zirconium-labeled monoclonal antibodies and their distribution in tumor-bearing nude mice. *J Nucl Med*. 1997;38:112–118.
32. Meijs WE, Haisma HJ, Van Der Schors R, et al. A facile method for the labeling of proteins with zirconium isotopes. *Nucl Med Biol*. 1996;23:439–448.
33. Perk L, Vosjan M, Visser G, et al. *p*-Isothiocyanatobenzyl-desferrioxamine: a new bifunctional chelate for facile radiolabeling of monoclonal antibodies with zirconium-89 for immuno-PET imaging. *Eur J Nucl Med Mol Imaging*. 2010;37:250–259.
34. Vosjan MJWD, Perk LR, Visser GWM, et al. Conjugation and radiolabeling of monoclonal antibodies with zirconium-89 for PET imaging using the bifunctional chelate *p*-isothiocyanatobenzyl-desferrioxamine. *Nat Protoc*. 2010;5:739–743.
35. Chopra A. <sup>89</sup>Zr-Labeled Trastuzumab, A Humanized Monoclonal Antibody Against Epidermal Growth Factor Receptor 2. Molecular Imaging and Contrast Agent Database (MICAD) [database online]. Bethesda, MD: National Library of Medicine, NCBI; 2004–2009; 2010. Available from: <http://micad.nih.gov>.
36. Dijkers ECF, Kosterink JGW, Rademaker AP, et al. Development and characterization of clinical-grade <sup>89</sup>Zr-trastuzumab for HER2/neu ImmunoPET imaging. *J Nucl Med*. 2009;50:974–981.
37. Dijkers E, Lub-de Hooge MN, Kosterink JG, et al. Characterization of <sup>89</sup>Zr-trastuzumab for clinical HER2 immunoPET imaging. *J Clin Oncol*. 2007;25(18S):3508.
38. Dijkers EC, Oude Munnink TH, Kosterink JG, et al. Biodistribution of <sup>89</sup>Zr-trastuzumab and PET Imaging of HER2-positive lesions in patients with metastatic breast cancer. *Clin Pharmacol Ther*. 2010;87:586–592.
39. Sampath L, Kwon S, Ke S, et al. Dual-Labeled trastuzumab-based imaging agent for the detection of human epidermal growth factor receptor 2 overexpression in breast cancer. *J Nucl Med*. 2007;48:1501–1510.
40. Perik PJ, Lub-De Hooge MN, Gietema JA, et al. Indium-111-labeled trastuzumab scintigraphy in patients with human epidermal growth factor receptor 2–positive metastatic breast cancer. *J Clin Oncol*. 2006;24:2276–2282.
41. Liu Y, Welch MJ. Nanoparticles labeled with positron emitting nuclides: advantages, methods, and applications. *Bioconjug Chem*. 2012;23:671–682.